

## Phase transition and ferroelectric properties of epitaxially strained $\text{KNbO}_3/\text{NaNbO}_3$ superlattice

Zhanfang Li,<sup>1,2</sup> Tianquan Lü,<sup>1</sup> and Wenwu Cao<sup>2,a)</sup><sup>1</sup>Department of Physics, Jilin University, Changchun 130023, China<sup>2</sup>Materials Research Institute, The Pennsylvania State University, University Park, Pennsylvania 16802, USA

(Received 16 October 2008; accepted 9 November 2008; published online 29 December 2008)

The influence of epitaxial strain on the crystal structure and polarization of  $\text{KNbO}_3/\text{NaNbO}_3$  (KNO/NNO) superlattice has been quantified using density functional theory based on pseudopotential and plane-wave basis. A sequence of structural phase transitions with changing the in-plane misfit strain has been identified. If the compressive strain is more than  $-0.8\%$ , tetragonal phase with polarization along  $[001]$  is stable. For the misfit strain between  $-0.8\%$  and  $0.36\%$ , the stable phase is monoclinic while the stable phase becomes orthorhombic with polarization along  $[110]$  when the tensile strain is more than  $0.36\%$ . The spontaneous polarization in the orthorhombic phase reaches more than  $70 \mu\text{C}/\text{cm}^2$ . © 2008 American Institute of Physics.  
[DOI: 10.1063/1.3053148]

Lead based piezoelectric ceramic  $\text{Pb}(\text{Zr}_{1-x}\text{Ti}_x)\text{O}_3$  (PZT) has been widely used in transducers, actuators, and sensors due to its excellent piezoelectric and electrical properties. However, because lead oxide vaporizes during the fabrication process, which is harmful to the environment, the development of lead-free ferroelectric materials with properties comparable to lead based compounds has become increasingly important. So far, several environmental friendly lead-free ferroelectric systems have been investigated. Among them,  $\text{K}_{0.5}\text{Na}_{0.5}\text{NbO}_3$  (abbreviated as KNN or NKN) is considered the most promising candidate because of its very high Curie temperature (above  $400^\circ\text{C}$ ), good ferroelectric properties ( $P_r=33 \mu\text{C}/\text{cm}^2$ ), and relatively large electromechanical coupling factors and relatively large piezoelectric coefficient  $d_{33}$ .<sup>1</sup> From what reported in the literature so far, all good lead-free piezoelectric are modified KNN system.

Ferroelectric superlattices composed of alternating epitaxial oxide ultrathin layers have intrigued great interest in recent years because they could produce very large polarization and good electric properties. With the rapid development of oxide thin film growth techniques such as molecular-beam epitaxy and pulsed laser deposition, it is now possible to fabricate artificial superlattices which can have new functionalities. For example, the artificial  $\text{BaTiO}_3/\text{SrTiO}_3$  superlattice exhibited very large dielectric constant.<sup>2-4</sup> It was also found that ferroelectricity as well as dielectric properties were enhanced with reducing the stacking periodicity.<sup>5,6</sup> Ferroelectricity was induced in  $\text{SrZrO}_3/\text{SrTiO}_3$  superlattice in spite of the paraelectric nature of  $\text{SrZrO}_3$  and  $\text{SrTiO}_3$ .<sup>7</sup> Because of the periodic nature, such superlattices can be easily studied using first principle's calculations. Based on previous theoretical studies, significant polarization enhancement can be achieved in ferroelectric superlattice in certain stacking sequence.<sup>8</sup> Epitaxial strain effect on properties of ferroelec-

tric superlattices has been also investigated for some systems.<sup>9-11</sup>

In this work, we report a quantitative first principle's analysis on the effect of in-plane misfit strain to the structural stability and ferroelectric properties of epitaxially grown  $(001) \text{KNO}_1 \text{ unit cell}/\text{NNO}_1 \text{ unit cell}$  superlattice. Our results indicate that there is a sequence of phase transitions with the change in the in-plane misfit strain, i.e., from tetragonal  $P4mm$  phase at high compressive strain to a monoclinic  $Cm$  phase with small misfit strain, and finally to an orthorhombic  $Amm2$  phase at larger tensile strain. The critical strain level at each phase boundary is determined by computing the Hessian matrix of each optimized structure. We have also calculated the change in polarization in each phase as a function of the misfit strain.

Our first principle's calculations on the crystal structure stability and polarization level of the KNO/NNO ferroelectric superlattice are based on the density functional theory (DFT) and density functional perturbation theory (DFPT)<sup>12-14</sup> within the local-density approximation (LDA),<sup>15,16</sup> which are implemented in the PWSCF package.<sup>17</sup> The interaction between nuclei and electrons was approximated using the Vanderbilt ultrasoft pseudopotentials<sup>18</sup> treating  $4s$ ,  $4p$ ,  $4d$ , and  $5s$  electrons of Nb,  $2s$  and  $2p$  electrons of O,  $2s$ ,  $2p$ , and  $3s$  electrons of Na, and  $3s$ ,  $3p$ , and  $4s$  electrons of K in the valence. A plane wave basis with kinetic energy cutoff of  $35 \text{ Ry}$  was used to represent wave functions, and Brillouin zone integrations were performed using a  $6 \times 6 \times 3$  Monkhost-pack  $k$ -point mesh.

For the prototypical cubic perovskite structure compounds  $\text{KNbO}_3$  and  $\text{NaNbO}_3$ , we determined the following values for the equilibrium lattice parameter:  $a(\text{KNbO}_3) = 7.467 \text{ a.u.}$ , ( $1 \text{ a.u.} = 0.529177 \text{ \AA}$ ), and  $a(\text{NaNbO}_3) = 7.394 \text{ a.u.}$ , comparable to the experimental values of  $7.604$  and  $7.427 \text{ a.u.}$ , respectively. Our results which compared very well with earlier DFT calculations are within the typical DFT-LDA errors in terms of lattice constant.

<sup>a)</sup>Electronic mail: dzk@psu.edu.

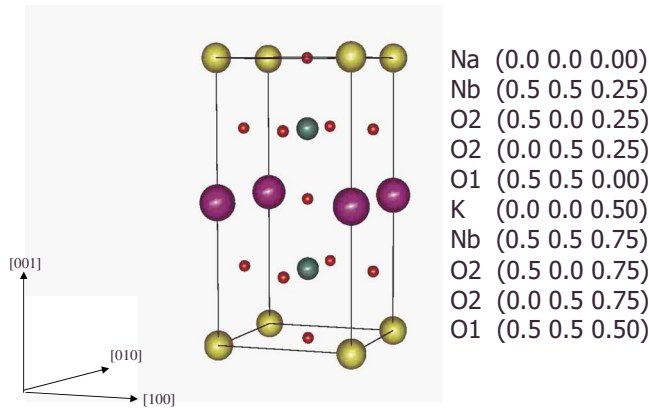


FIG. 1. (Color online) Atomic positions in a ten-atom unit cell of an ideal double-perovskite  $\text{KNbO}_3/\text{NaNbO}_3$  superlattice with centrosymmetric crystal structure.

The epitaxial constraint from a cubic substrate was represented by changing the in-plane lattice constant of the superlattice. We used in-plane lattice parameter deviation from  $a_0=7.43$  a.u. to define the epitaxial strain, where  $a_0$  was obtained by energy minimization of the centrosymmetric crystal structure of  $\text{KNO}/\text{NNO}$  superlattice. To study the effects of epitaxial strain, we varied the in-plane lattice constant from  $a_0-0.12$  to  $a_0+0.12$  a.u., allowing all atomic positions and the out-of-plane lattice constant to relax fully until the total energy is minimized. The misfit strain of the superlattice is represented by

$$\eta(\%) = \frac{a - a_0}{a_0} \times 100(\%).$$

For each value of the epitaxial strain, we investigated three types of low-symmetry ferroelectric structures: a tetragonal phase (space group  $P4mm$ , No. 99) with polarization  $P_z$  along  $[001]$ , an orthorhombic phase (space group  $Amm2$ , No. 38) with polarization  $P_{(x+y)}$  along  $[110]$ , and a monoclinic phase (space group  $Cm$ , No. 8) with a combined polarization given by two components,  $P_{(x+y)}$  along  $[110]$  and  $P_z$  along  $[001]$ . The stability limit of each crystal structure was evaluated through the calculation of zone-center phonon modes using DFPT because the total energy difference is too small near the phase boundary. The polarization  $|\mathbf{P}|$  for each stable structure was calculated using the linearized expression

$$P_\alpha = \frac{e}{\Omega} \sum_{i\beta} Z_{i,\alpha\beta}^* u_{i\beta},$$

where  $u_{i\beta}$  is the atomic displacement relative to the ideal double-perovskite ten-atom unit cell, as shown in Fig. 1,  $Z_{i,\alpha\beta}^*$  is the atomic Born effective charge tensor computed using DFPT,  $e$  is the absolute value of the electron charge, and  $\Omega$  is the unit cell volume.

In Fig. 2, we show the total energy of the superlattice as a function of the misfit strain. The energy of the tetragonal superlattice is the lowest when the compressive strain is beyond  $-0.8\%$ , whereas the energy of the orthorhombic superlattice is the lowest when the tensile strain is larger than  $0.36\%$ . For the misfit strain level between  $-0.8\%$  and  $0.36\%$  the stable phase is monoclinic, whose polarization vector can

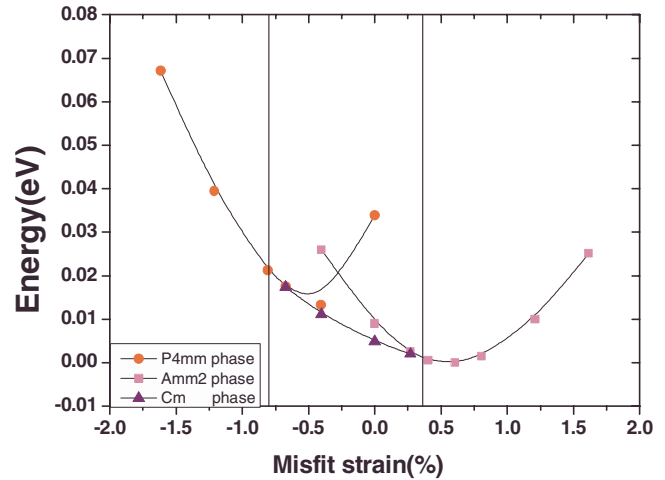


FIG. 2. (Color online) The total energy of  $\text{KNbO}_3/\text{NaNbO}_3$  superlattices as a function of misfit strain for tetragonal, orthorhombic, and monoclinic structures.

be decomposed into tetragonal and orthorhombic components so that the misfit strain induced phase transition can be viewed as the rotation of the polarization from  $[001]$  to  $[110]$ . Because the differences of total energy at the phase boundaries are too small to be used to define the  $P4mm$ - $Cm$  and  $Cm$ - $Amm2$  phase boundaries, the stability of the zone-center optical phonon mode is utilized for this purpose, which becomes soft at the misfit strain driven phase transitions.

Figure 3 shows the polarization of the  $\text{KNO}/\text{NNO}$  superlattice as a function of the misfit strain. The symmetry change is evident from the rotation of the polarization from  $[001]$  to  $[110]$ . If the compressive strain is more than  $-0.8\%$ , the stable tetragonal phase has a polarization along the direction normal to the stacking planes of the superlattice and it reduces as the absolute value of the strain is reduced. When the compressive strain is reduced below the critical value of  $-0.8\%$ , the crystal structure becomes monoclinic and the polarization component along  $[001]$  continues to reduce with the misfit strain increasing toward positive value. The polarization component along  $[110]$  starts to appear at the tetragonal-monoclinic phase boundary and increases as the misfit strain increases, while the total polarization also in-

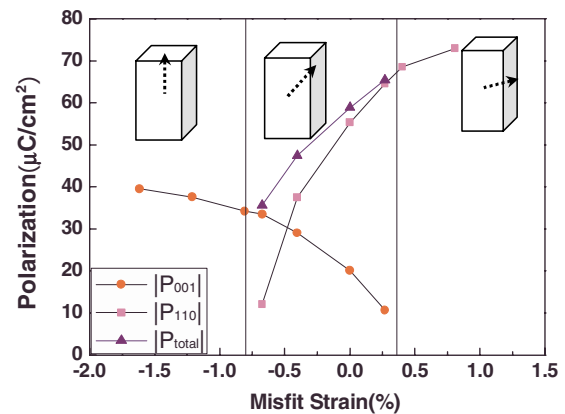


FIG. 3. (Color online) Polarization amplitude of  $\text{KNO}/\text{NNO}$  superlattice as a function of misfit strain.

creases. This trend continues as the misfit strain becomes tensile-type until it reaches another critical value of 0.36%, at which the tetragonal polarization component completely vanishes and the stable crystal structure becomes orthorhombic with a polarization along [110]. The polarization amplitude continues to increase with increase in in-plane misfit strain and reaches more than  $70 \mu\text{C}/\text{cm}^2$  in the orthorhombic phase, as shown in Fig. 3.

Our results imply that the KNO/NNO superlattice will be under compressive strain and have a tetragonal structure with polarization along [001] if it is grown epitaxially onto a substrate whose in-plane lattice constant is smaller than  $a_0$  by 0.8%. With the increase in the in-plane lattice constant of the substrate, the misfit becomes smaller and the stable crystal structure will become monoclinic  $Cm$  phase. When the lattice constant of the substrate is larger than  $a_0$  by 0.36%, the superlattice is subjected to a tensile stress and the stable crystal structure will become orthorhombic  $Amm2$ . The net polarization rotates gradually from [001] to [110] with the change in misfit strain from compressive-type to tensile-type.

In summary, we have obtained the phase diagram of KNO/NNO superlattice with respect to the change in the misfit strain based on first principle's calculations. The superlattice system is tetragonal with the polarization along [001] ( $P4mm$  symmetry) when the amplitude of the compressive strain is more than 0.8% and is orthorhombic with polarization along [110] ( $Amm2$  symmetry) when the tensile strain is more than 0.36%. For the misfit strain level between  $-0.8\%$  and  $0.36\%$ , the monoclinic phase ( $Cm$  symmetry) is stable and the polarization contains both [001] and [110]

components. It is interesting to note that the polarization reaches more than  $70 \mu\text{C}/\text{cm}^2$  in the orthorhombic phase, which is 80% higher than that in the tetragonal phase.

Financial support for this work was provided by the NIH under Grant No. P41-EB21820. One of the authors (Z.L.) acknowledges the financial support from the Chinese Ministry of Education of the People's Republic of China for the joint-training Ph.D. student program.

- <sup>1</sup>D. Lin, K. W. Kwok, K. H. Lam, and H. L. W. Chan, *J. Appl. Phys.* **101**, 074111 (2007).
- <sup>2</sup>H. Tabata, H. Tanaka, and T. Kawai, *Appl. Phys. Lett.* **65**, 1970 (1994).
- <sup>3</sup>J. Lee, L. Kim, J. Kim, D. Jung, and U. V. Waghmare, *J. Appl. Phys.* **100**, 051613 (2006).
- <sup>4</sup>L. Kim, D. Jung, J. Kim, Y. S. Kim, and J. Lee, *Appl. Phys. Lett.* **82**, 2118 (2003).
- <sup>5</sup>T. Wu and C. Hung, *Appl. Phys. Lett.* **86**, 112902 (2005).
- <sup>6</sup>C.-L. Hung, Y.-L. Chueh, T.-B. Wu, and L.-J. Chou, *J. Appl. Phys.* **97**, 034105 (2005).
- <sup>7</sup>T. Tsurumi, T. Harigai, D. Tanaka, S. M. Nam, H. Kakemoto, S. Wada, and K. Saito, *Appl. Phys. Lett.* **85**, 5016 (2004).
- <sup>8</sup>B. Neaton and K. M. Rabe, *Appl. Phys. Lett.* **82**, 1586 (2003).
- <sup>9</sup>C. Bungaro and K. M. Rabe, *Phys. Rev. B* **69**, 184101 (2004).
- <sup>10</sup>L. Kim, J. Kim, D. Jung, and J. Lee, *Appl. Phys. Lett.* **87**, 052903 (2005).
- <sup>11</sup>L. Kim and J. Kim, *Phys. Rev. B* **72**, 214121 (2005).
- <sup>12</sup>P. Hohenberg and W. Kohn, *Phys. Rev.* **136**, B864 (1964).
- <sup>13</sup>W. Kohn and L. J. Sham, *Phys. Rev.* **140**, A1133 (1965).
- <sup>14</sup>S. Baroni, S. Gironcoli, A. D. Corso, and P. Giannozzi, *Rev. Mod. Phys.* **73**, 515 (2001).
- <sup>15</sup>D. M. Ceperley and B. J. Alder, *Phys. Rev. Lett.* **45**, 566 (1980).
- <sup>16</sup>J. P. Perdew and A. Zunger, *Phys. Rev. B* **23**, 5048 (1981).
- <sup>17</sup>S. Baroni, A. Dal Corso, S. de Gironcoli, and P. Giannozzi, <http://www.pwscf.org>.
- <sup>18</sup>D. Vanderbilt, *Phys. Rev. B* **41**, 7892 (1990).